Channel Estimation in STBC-OFDM Systems

Final Project Report

Detection and Estimation Theory

ECEN-5652

by

Vishal Srivastav

Department of Electrical Engineering
University of Colorado, Boulder
USA - 80302
May 2017

Abstract

Orthogonal Frequency Division Multiplexing is a multi-carrier transmission scheme that uses overlapping subcarriers. It essentially converts a frequency selective channel to a set of parallel flat fading channels.

Space Time Block Coding is a diversity scheme that employs spatial diversity. In this scheme multiple copies of the datastream are transmitted from different antennas so that some of the copies arrive at the receiver in a better state.

In this project, the STBC OFDM communication system which merges together the properties of the above mentioned schemes was studied. The system was designed and performance comparisons were done using BER plots assuming perfect CSI knowledge. All the simulations were done in a fading channel environment. To generate this channel, Modified Smiths Method was used. Then various classes of channel estimators were studied which included LS, MMSE(Wiener Filter). These estimators were first employed in a SISO OFDM system and then ported to the STBC OFDM system. Performance of these schemes were evaluated both from the NMSE and BER plots.

Application of Kalman Filter for channel estimation in STBC OFDM systems was done to obtain an improvement on the existing estimators. As Kalman Filter required an AR process as its state function, the AR approximation for a fading channel was studied and implemented. Better performance with respect to NMSE and BER was observed.

TABLE OF CONTENTS

CHAPTER 1

Introduction and Problem Statement

1.1 Introduction

In a basic wireless communication system, the data is modulated on to a single carrier frequency. The available bandwidth is totally occupied by each symbol. But transmission rates are severely limited in a single carrier environment due to Inter Symbol Interference (ISI). ISI occurs when the symbol time is comparable to the channel delay spread. This sets the upper limit for transmission rate in the single carrier system. Hence we require multicarrier transmission schemes.

In multicarrier transmission scheme total bandwidth available to the system is divided into a series of frequency sub-bands. The data is then sent in parallel through these sub-bands. Orthogonal Frequency Division Multiplexing (OFDM) is a type of multicarrier scheme that improves the bandwidth efficiency of the system. Basic idea behind OFDM is to divide the available spectrum into several orthogonal subcarriers. By doing so the spectrum of subcarriers overlap thereby increasing the bandwidth efficiency and also, each narrowband sub-channels experience almost flat fading thereby increasing the reliability. A way to minimize Inter Block Interference (IBI) in OFDM is to use Cyclic Prefix (CP).

In OFDM systems, we can further increase reliability by implementing Space Time Block Coding (STBC).

Channel estimation and equalization is an integral part of OFDM system design. For proper decoding of the signal at the receiver accurate channel state information is necessary. Often channel state information is obtained by transmitting known training sequence as pilot symbols. A conventional communication system receiver, first obtain the channel estimates at the of the pilot symbols using various algorithms like LS, MMSE, Kalman filtering, etc, which is interpolated and used for decoding the received signal.

1.2 Problem Statement

The main objective of this project was to implement a recursive channel estimation technique(Kalman Filtering) to STBC OFDM systems to get more accurate channel estimates compared to existing techniques. In this project we studied the existing techniques of LS and MMSE. The Kalman Filtering based approach for SISO model was also studied. A comparison between the various techniques were also done to see the improvement achieved by using Kalman Filters. Then this concept was extended to STBC OFDM systems and again a comparison between the existing LS technique and proposed Kalman techniques was done.

CHAPTER 2

Space-Time Block Coded OFDM Systems

2.1 Introduction

The combination of OFDM and STBC techniques seems to offer a very promising ground for the research targeted for high data-rate communication systems. In this chapter we will discuss the system model for the STBC-OFDM communication systems.

2.2 System Model

A simplified block diagram of space-time block coded OFDM system has been presented in Figure 2.1 which has I transmitter antennas and J receiver antennas. At the transmitter, first signal is modulated using any modulator of our choice, the modulated signal is denoted by $S(k,n)$. Now $S(k,n)$ is fed to space-time block coder which converts the signal into several parallel information streams. The space-time coding is done in a way that the input symbols of the coder correspond to the subcarriers in adjacent OFDM symbols. Now these space time coded symbols is converted into OFDM symbols by applying IFFT, and then a cyclic prefix is added to the beginning of each OFDM symbol.

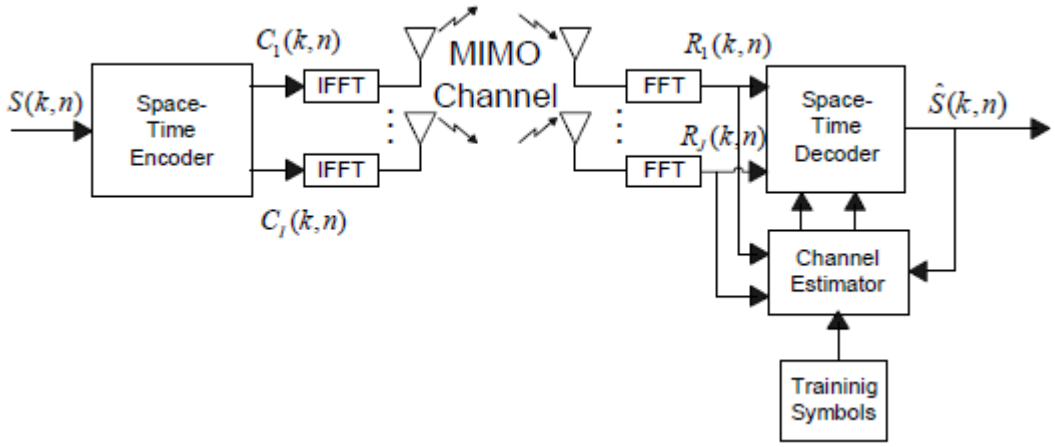

Figure 2.1: Basic block diagram of space-time block coded OFDM system [8]

At the receiver, first the cyclic prefix is removed and then FFT is applied. For this model we have assumed perfect synchronization and that the cyclic prefix is longer than the channel delay spread. So then the received signal at antenna j can be written as:

$$R_j(k.n) = \sum_{i=1}^{I} H_{ij}(k,n)C_i(k,n) + n_j(k,n) \tag{2.1}$$

where n is the OFDM symbol number and k is the subcarrier index. $H_{ij}(k,n)$ the k-th subcarrier component of the channel transfer function between the i-th and j-th antennas. $C_i(k,n)$ represents the modulated symbol and $n_j(k,n)$ is the complex additive white Gaussian noise (AWGN) of variance σ_j^2. This signal is then given to the channel estimator which uses the embedded pilot tones within the signal to get the channel estimates. The channel information and the received signal is given as input to the space-time decoder from which the received signal is decoded and the transmitted symbols are recovered.

2.3 Results

2.3.1 Simulation Parameters

- Modulation Scheme: 16 QAM
- FFT Size: 256
- Cyclic Prefix: 32
- Channel PDP: [0, -8, -17, -21, -28] dB

2.3.2 Effect of increasing Transmit Antennas

The following simulation was done for an STBC-OFDM system of code rate=0.5 and number of receive antennas, $N_r = 2$ in a slow fading Rayleigh channel.

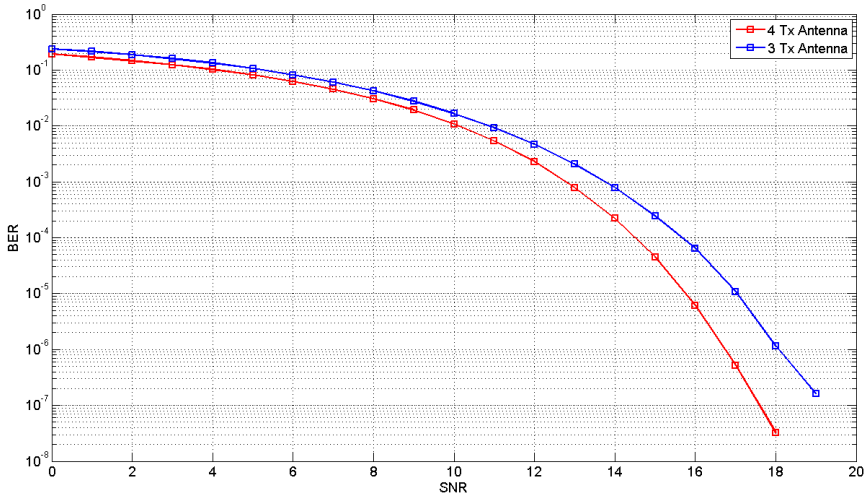

Figure 2.2: Effect of increasing the number of transmit antennas

Inference

From Figure 2.2 we can see that on increasing the number of transmit antennas we get a better BER result.

2.3.3 Effect of increasing Receive Antennas

The following simulation was done for an STBC-OFDM system of code rate=0.75 and number of transmit antennas, $N_t = 4$ in a slow fading Rayleigh channel.

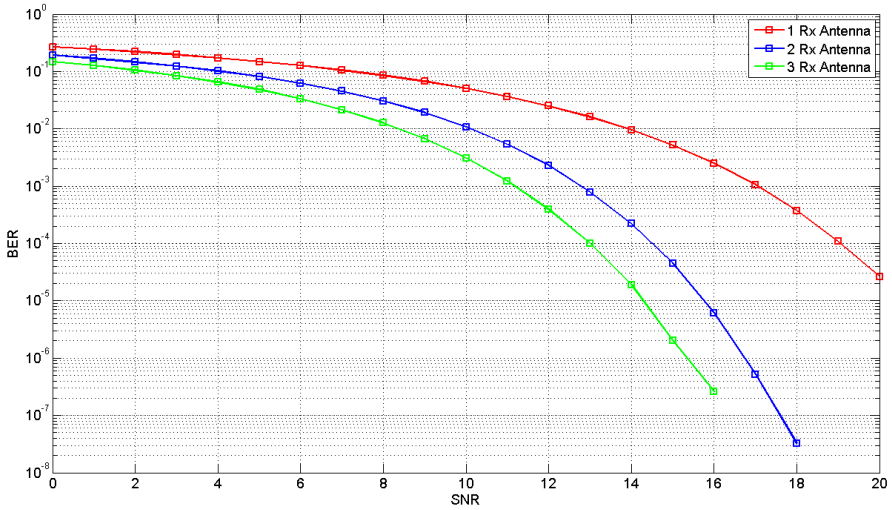

Figure 2.3: Effect of increasing the number of receive antennas

Inference

From Figure 2.3 we can see that on increasing the number of receive antennas we get a better BER result.

2.3.4 Effect of increasing Code Rate

STBC-OFDM system transmit antennas, $N_t = 4$ and receive antennas, $N_r = 2$ in a slow fading Rayleigh channel.

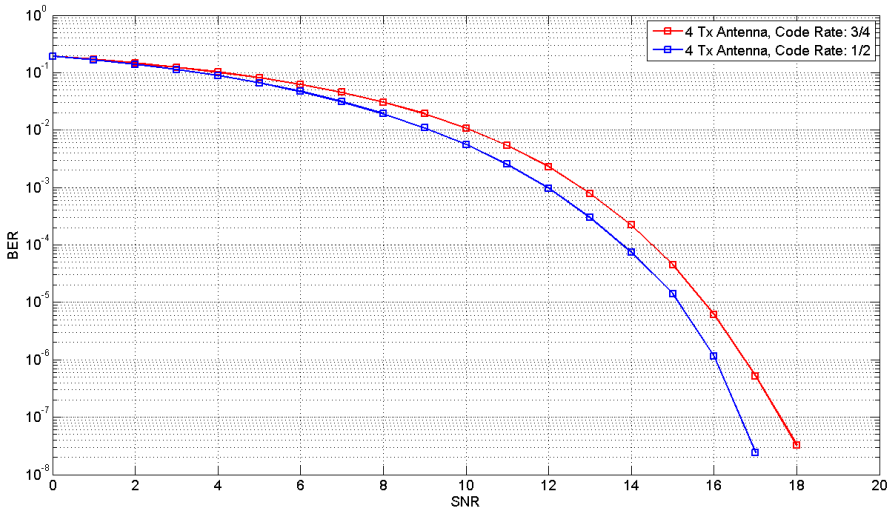

Figure 2.4: Effect of increasing the code rate

Inference

From Figure 2.4 we can see that on increasing code rate, the performance deteriorates.

CHAPTER 3

Fading Channels

3.1 Introduction

Based on excess delay of the channel τ_m and symbol duration T_{sym} fading can be characterised as follows

1. Flat Fading
2. Frequency Selective Fading

When maximum excess delay of the channel is less than symbol period i.e. $\tau_m < T_{sym}$ maximum delay the channel can offer will always be less than one symbol period so all the multipath components of the symbol arrive during the same signalling interval and there will not be any significant interference between adjacent symbols at the receiver. Such a channel is called Flat Fading Channel.

Now if Now if $\tau_m > T_{sym}$, the channel exhibits frequency selective fading where excess delay by the channel can exceed one symbol period. In such a case, some of the multipath components of n^{th} transmitted symbol can arrive during $(n+1)^{th}$ symbol duration. This results in Inter Symbol Interference (ISI). In frequency selective channel the gain of the channel is different for different frequency components.

In the frequency domain, Doppler spread characterizes the effect of time varying nature of the channel on the received signal. The Doppler shift in the frequency of each of the multipath waves arises due to the motion of transmitter and receiver. The amount of Doppler shift will be different for each of the multipath waves as the angle of arrival of each wave is randomly distributed. This results in spectral broadening of the signal. The amount of spectral broadening is expressed in terms of Doppler spread. The Doppler spread, f_d, is the maximum Doppler shift and is given by,

$$f_d = \frac{v}{\lambda} \tag{3.1}$$

where v is the velocity of relative motion between transmitter and receiver in meters/second and λ is the wavelength of the signal in meters.

3.2 Clarke's Mathematical Model of Flat Fading Channel

A mathematical model was generated by clarke for flat fading channel. Assumption taken in this particular model are:

1. Fixed transmitter(vertically polarized antenna) and receiver moving with velocity v
2. No direct path(i.e.no line of sight path)
3. N multipath components arriving at random angles at the receiver.

As flat fading channel is taken in consideration so it is assumed that all the waves arrive at the same time at the receiver. The Doppler shift f_n on the n^{th} wave, arriving at an angle α_n, is

$$f_n = \frac{v}{\lambda} cos\alpha_n \tag{3.2}$$

where λ is the wavelength of the incident wave (meters), α_n is uniformly distributed over $[0, 2\pi]$

Let $x(t) = cos(2\pi f_c t)$ be the transmitted signal. The received signal can $y(t)$ can be expressed as,

$$y(t) = \sum_{i=1}^{N} a_i cos(2\pi f_c t + 2\pi f_i t + \theta_i) \tag{3.3}$$

Where, N is the total number of paths, a_i is the attenuation coefficient of i^{th} path, θ_i is the phase shift of the i^{th} path, and f_i is the Doppler shift of the i^{th} multipath component

We can also express y(t) as sum of in-phase and quadrature-phase components, I(t) and Q(t) respectively:

$$y(t) = I(t)cos(2\pi f_c t) + Q(t)sin(2\pi f_c t) \tag{3.4}$$

Where,

$$I(t) = \sum_{i=1}^{N} a_i cos(2\pi f_i t + \theta_i) \tag{3.5}$$

$$Q(t) = \sum_{i=1}^{N} a_i sin(2\pi f_i t + \theta_i) \tag{3.6}$$

For large number of paths between transmitter and receiver, I(t) and Q(t) can be approximated as Gaussian random variables with zero mean and variance σ^2 [9] then, the envelope R(t) of the received signal will be,

$$R(t) = \sqrt{I(t)^2 + Q(t)^2} \tag{3.7}$$

As I(t) and Q(t) are Gaussian and independent of each other, R(t) can be shown to have Rayleigh distribution [6]. The probability density function (pdf) of R(t) is given by

$$f_R(r)(r) = \begin{cases} \frac{r}{\sigma^2} e^{-\frac{r^2}{2\sigma^2}} & \text{r} \geq 0 \\ 0 & \text{r} < 0 \end{cases}$$

In frequency domain power spectrum of received fading signal as defined in Clarke's model has the U shaped bandlimited form:

$$S(f) = \begin{cases} \frac{1}{\pi f_d \sqrt{1-(\frac{f-f_c}{f_d})^2}} & |f - f_c| \leq f_d \\ 0 & \text{elsewhere} \end{cases}$$

where f represents the frequency in Hertz, f_c is the carrier frequency and f_d is the maximum Doppler frequency. The equivalent autocorrelation function in time domain of the received signal is given by

$$r(\tau) = J_0(2\pi f_d \tau) \tag{3.8}$$

where $J_0(.)$ is the zeroth order Bessel function of the first kind, and τ is the separation between observation times in seconds.

3.3 Simulation Algorithms of Flat Fading Channel

3.3.1 Smith's Simulator

To simulate the mathematical model we first have to generate zero mean complex Gaussian sequence which can be generate as given in Figure 3.1.

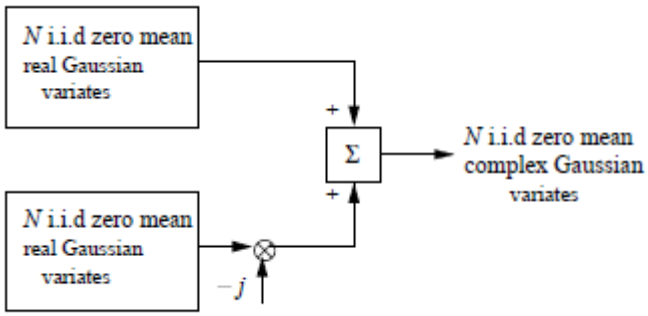

Figure 3.1: Generation of complex Gaussian sequence

As shown in Figure 3.1, complex Gaussian variables can be created by first generating two real Gaussian sequence, multiplying $-j$ to one of the branch and then adding them together.

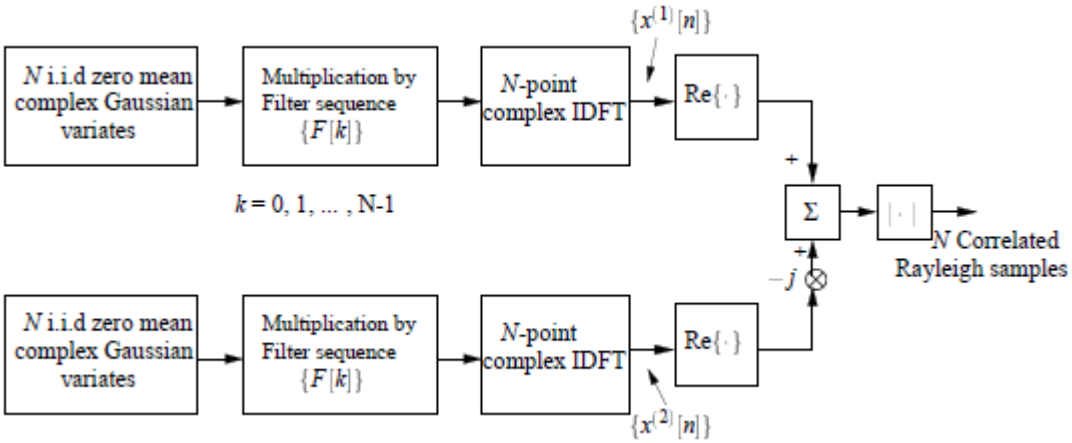

Figure 3.2: Block diagram of Smith's simulator

As show in Figure 3.2, after generating the zero mean complex Gaussian sequence, it is multiplied by an appropriate filter sequence $F|k|$ for shaping the Gaussian sequence to a desired U shaped power spectrum. The filter coefficients of $F|k|$ are discrete frequency representation of $S(f)$. After this complex Gaussian sequence is converted into time domain by an IDFT operation. Finally we got complex time Gaussian sequence with desired auto correlation properties. But the real and imaginary part of $(x^{(1)}[n])$ are correlated. To get the uncorrelated real and imaginary parts $Re(x^{(1)}[n])$ is added in quadrature with another complex Gaussian sequence denoted by $(x^{(2)}[n])$ which is generated by second identical but independent branch. The magnitude of $(x^{(1)}[n])+j(x^{(2)}[n])$ will give us desired Rayleigh sequence representing the samples of time domain fading waveform.

3.3.2 Modification to Smith's Algorithm

A modified version of smith's algorithm was presented by D.J young and N.C Beaulieu [11], which enables the generation of correlated Rayleigh random variables using single IDFT operation. Figure 3.3 shows how we can generate complex Rayleigh sequence by single IDFT operation

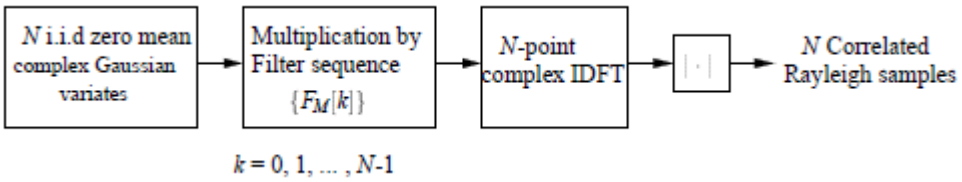

Figure 3.3: Rayleigh sequence generation with single IDFT operation

As we can see in above Figure 3.3 the modification has been done in Filter sequence. Modified filter $F_M[k]$ sequence ensures that output of a single IDFT operation will give uncorrelated real and imaginary parts, hence there is no need of second branch (IDFT operation). This results in significant reduction in computational complexity of smith's algorithm.

The modified filter$F_M(k)$ which is used to shape the random Gaussian variables to get desired U shaped doppler power spectrum is

$$F_M(k) = \begin{cases} 0 & k = 0 \\ \sqrt{\frac{1}{2\sqrt{1-(\frac{k}{Nf_m})^2}}} & k = 1, 2, ...k_m - 1 \\ \sqrt{\frac{k_m}{2}[\frac{\pi}{2} - \arctan(\frac{k_m - 1}{\sqrt{2k_m - 1}})]} & k = k_m \\ 0 & k = k_m + 1, ..., N - k_m - 1 \\ \sqrt{\frac{k_m}{2}[\frac{\pi}{2} - \arctan(\frac{k_m - 1}{\sqrt{2k_m - 1}})]} & k = N - k_m \\ \sqrt{\frac{1}{2\sqrt{1-(\frac{N-k}{Nf_m})^2}}} & k = N - k_m + 1, ...N - 2, N - 1 \end{cases}$$

Where,
N=Number of correlated Rayleigh samples to be generated
$f_m = \frac{f_d}{f_s}$ = normalized Doppler frequency
f_d=Maximum Doppler frequency
f_s = Sampling frequency
$k_m = f_m N$

k_m is the point at or just below, the maximum Doppler frequency. The filter coefficient at k_m is chosen such that the area under an interpolation of the spectrum coefficients is equal to the area under the continuous-time spectrum curve given by S(f).

3.4 Auto regressive Model for Fading Channel Simulation [12]

The IDFT technique discussed above is a high quality and efficient fading generator. But the disadvantage of this method is that all the samples are generated in a single

FFT operation. Therefore to generate a very large number of samples, the memory requirement for this method makes it unattractive. In this section we describe the use of a general auto regressive (AR) modeling approach for the generation of correlated Rayleigh samples.

3.4.1 Generation

As discussed before, the theoretical power spectral density of either the in-phase or quadrature phase part of the received fading signal has the U shaped bandlimited form:

$$S(f) = \begin{cases} \frac{1}{\pi f_d \sqrt{1-(\frac{f}{f_d})^2}} & |f| \leq f_d \\ 0 & \text{elsewhere} \end{cases}$$

Here f_d is the maximum Doppler shift in Hertz. The equivalent normalized continuous time autocorrelation of the received signal is $R(\tau) = J_0(2\pi f_d \tau)$, here $J_0(.)$ is the zeroth order Bessel function of the first kind. For the discrete time scenario, theoretically, the generated in-phase and quadrature Gaussian processes should each have the autocorrelation sequence: $R[n] = J_0(2\pi f_m |n|)$ Here, $f_m = f_d/F_s$ is the maximum Doppler shift normalized by the sampling rate F_s. Also the in-phase and quadrature processes must be independent and each must have zero mean for Rayleigh fading.

3.4.2 AR Modeling

A complex p-th order AR process can be generated by the time domain recursion

$$x[n] = -\sum_{k=1}^{p} a_k x[n-k] + w[n] \tag{3.9}$$

Where $w[n]$ is a complex white Gaussian noise process with uncorrelated real and imaginary parts. For Rayleigh modeling w[n] should have zero mean. The AR model parameters that need to be found are the coefficients $a_1, a_2, , a_p$ and the variance σ_p^2 of $w[n]$. The Power Spectral Density of this model has the rational form given by

$$S(f) = \frac{\sigma_p^2}{|1 + \sum_{k=1}^{p} a_k exp(-j2\pi fk)|^2} \tag{3.10}$$

Although the theoretical spectrum is not rational, an AR model of sufficiently high order can closely approximate the theoretical spectrum.

$$R_{xx}[k] = \begin{cases} -\sum_{m=1}^{p} a_m R_{xx}[k-m] & \text{if } k \geq 1 \\ -\sum_{m=1}^{p} a_m R_{xx}[-m] + \sigma_p^2 & \text{if } k = 0 \end{cases}$$

In matrix form this can be written as: $\mathbf{R_{xx}a} = -\mathbf{v}$
Here,

$$\mathbf{R_{xx}} = \begin{bmatrix} R_{xx}[0] & R_{xx}[-1] & ... & R_{xx}[-p+1] \\ R_{xx}[1] & R_{xx}[0] & ... & R_{xx}[-p+2] \\ . & . & . & . \\ . & . & . & . \\ . & . & . & . \\ R_{xx}[p-1] & R_{xx}[p-2] & ... & R_{xx}[0] \end{bmatrix}$$

$\mathbf{a} = [a_1, a_2, , a_p]^T$, $\mathbf{v} = [R_{xx}[1], R_{xx}[2], , R_{xx}[p]]^T$

and $\sigma_p^2 = R_{xx}[0] + \sum_{k=1}^{p} a_k R_{xx}[k]$

So given the required ACF sequence, the AR filter coefficients can be determined by solving the p equations given above. And these set of equations are called Yule-Walker equations.

As $\mathbf{R_{xx}}$ is an autocorrelation matrix, it is positive semidefinite and can be shown to be singular only if the process is purely harmonic and consists of p-1 or fewer sinusoids. In all other cases these equations are guaranteed to have a unique solution for $\mathbf{a}$. The generated AR process has its ACF given by,

$$\hat{R}_{xx}[k] = \begin{cases} R_{xx}[k] & \text{if } 0 \leq k \leq p \\ -\sum_{m=1}^{p} a_m \hat{R}_{xx}[k-m] & \text{if } k > p \end{cases}$$

That is the generated process has the nice property that its sampled ACF perfectly matches with the desired ACF up to a lag of p.

3.5 Results

3.5.1 Simulation of Flat Fading Channels by Single IDFT Algorithm

Fading Signal Envelope

Figure 3.4 to Figure 3.7 show the results when four different fade rates, 1Hz, 10Hz, 100Hz and 1000Hz, are simulated using the single IDFT method. For each simulation, the time varying envelope of the fading signal has been plotted.

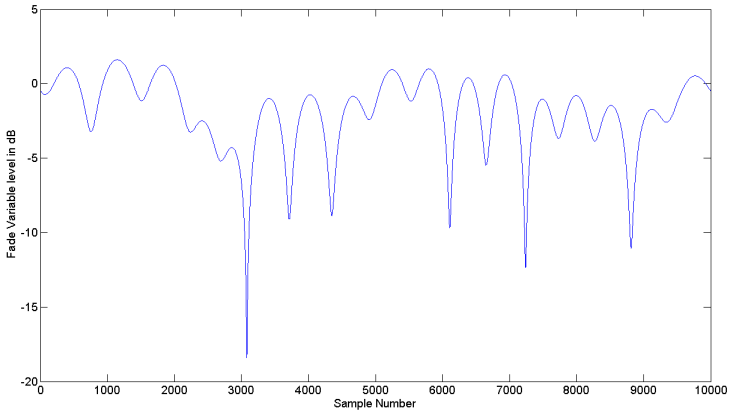

Figure 3.4: Simulated Fading Signal Envelope, $f_d = 1Hz$

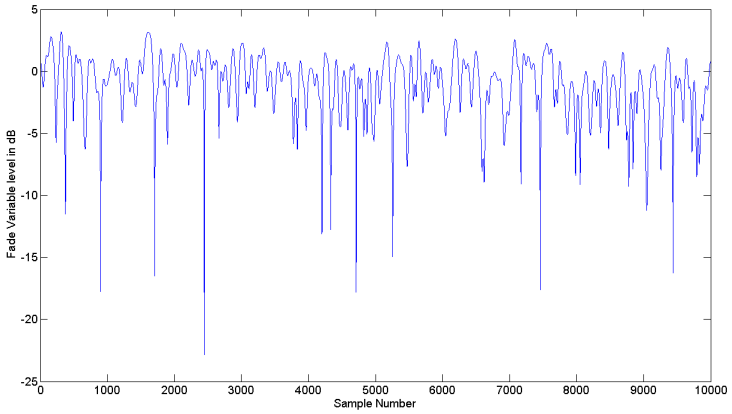

Figure 3.5: Simulated Fading Signal Envelope, $f_d = 10Hz$

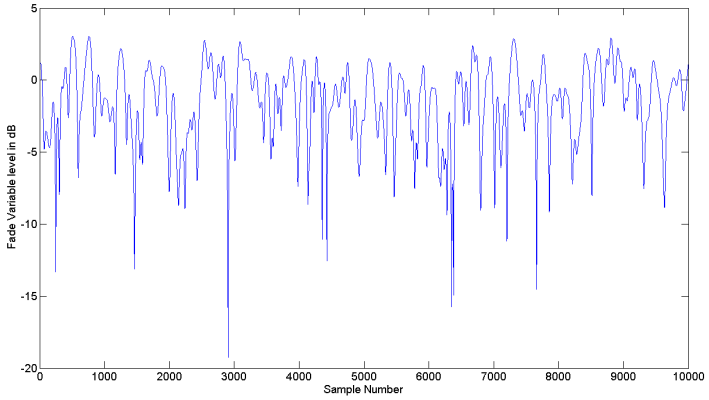

Figure 3.6: Simulated Fading Signal Envelope, $f_d = 100Hz$

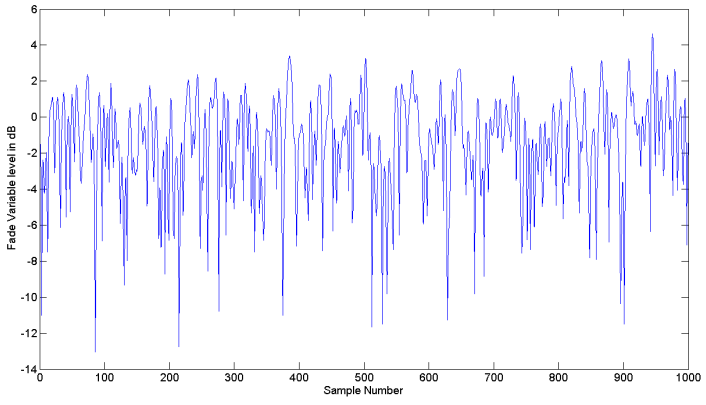

Figure 3.7: Simulated Fading Signal Envelope, $f_d = 1000Hz$

Inference

As the doppler frequency increases the rate at which the magnitude of the fade variable changes also increases. This is to be expected because when the vehicle moves at a higher velocity the channel also changes at a higher rate.

3.5.2 Simulation of Flat Fading Channels by AR Modeling

Autocorrelation Sequence of AR Model

Figure 3.8 shows the autocorrelation sequence plotted for the AR models of different orders as well as for the original fading channel.

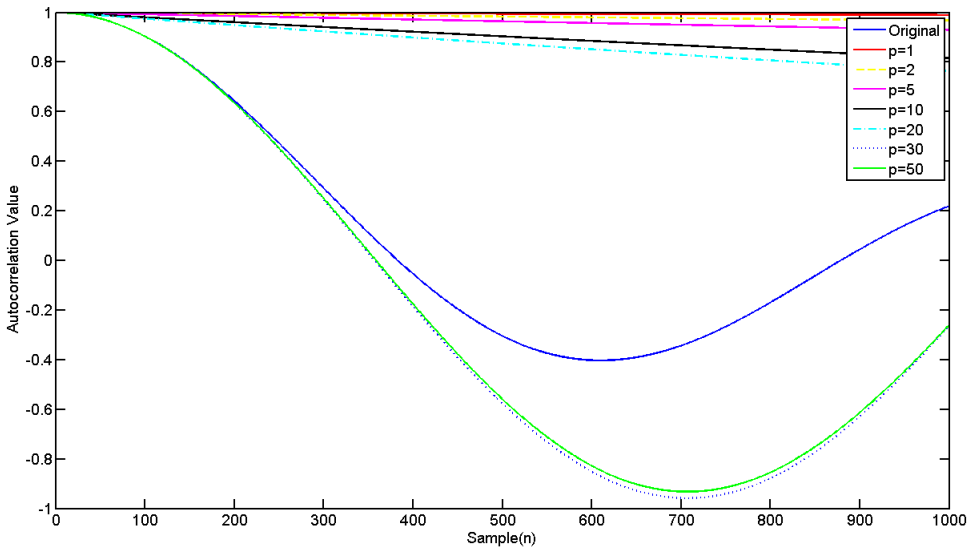

Figure 3.8: Autocorrelation Function of actual fading channel and AR approximations of various orders

Inference

We can clearly see from Figure 3.8 that as we increase the order we get a closer approximation to the actual model. Also, the ACF of the p^{th} order approximate matches with the actual ACF till the p^{th} lag.

Pole Zero Plots of the Transfer Function

Figure 3.9 to Figure 3.11 shows the pole zero plots for various orders of the AR model transfer function.

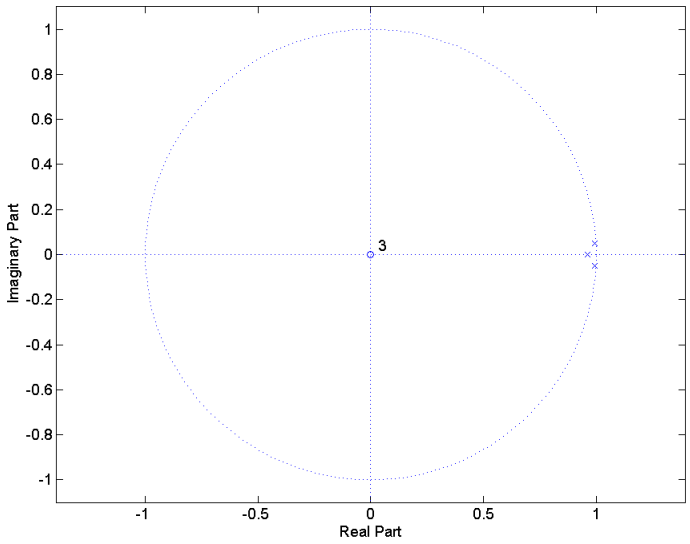

Figure 3.9: Pole Zero Plot for p=3

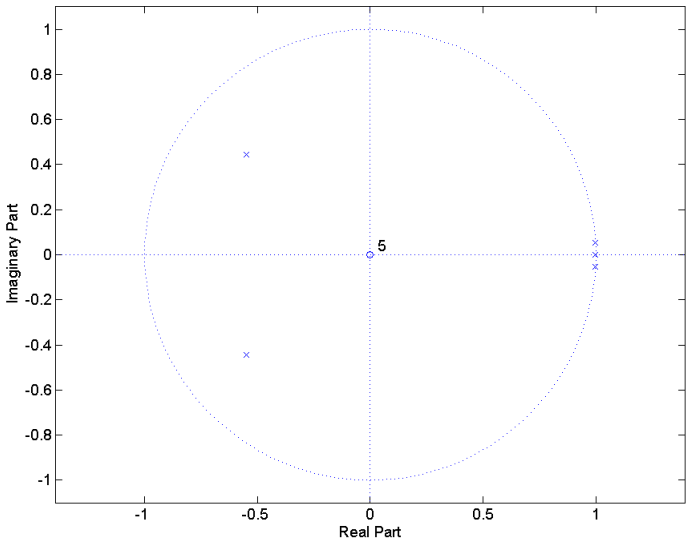

Figure 3.10: Pole Zero Plot for p=5

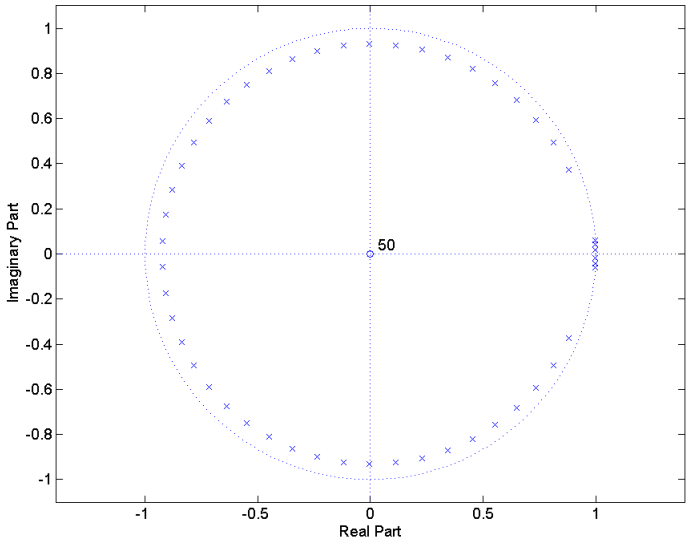

Figure 3.11: Pole Zero Plot for p=50

Inference

From the above figures we can see that the poles always lies within the unit circle. Hence we can conclude that the system is always stable.

CHAPTER 4

Channel Estimation

4.1 Introduction

In OFDM system each subcarrier can be considered as separate channel. The orthogonality between subcarriers allows us to define received signal as product of transmitted signal and channel response, thus transmitted signal can be recovered by estimating the channel response at each subcarrier in the receiver. Generally preamble or pilot symbols known to both transmitter and receiver are used to estimate the channel, which employ various interpolation techniques to estimate the channel response of the subcarriers between pilot tones. During choosing the channel estimation technique in OFDM system computational complexity of the technique and time-variation of the channel should be considered.

4.2 System Definition

As we know from previous chapters that all the subcarriers in OFDM system are orthogonal to each other. Considering this property we can represent the training symbols for N subcarriers in the form of diagonal matrix:

$$X = \begin{bmatrix} X[0] & \cdots & \cdots & 0 \\ 0 & X[1] & \cdots & 0 \\ \vdots & \vdots & \ddots & \vdots \\ 0 & 0 & \cdots & X[N-1] \end{bmatrix}$$

Where X[k] denotes a pilot tone at k^{th} subcarrier, $k = 0, 1, 2, .N-1$. Given that channel gain is H[k] for each subcarrier k, the received signal Y[k] can be defined as

$$\begin{bmatrix} Y[0] \\ Y[1] \\ \vdots \\ Y[N-1] \end{bmatrix} = \begin{bmatrix} X[0] & 0 & \cdots & 0 \\ 0 & X[1] & \cdots & 0 \\ \vdots & \vdots & \ddots & \vdots \\ 0 & 0 & \cdots & X[N-1] \end{bmatrix} \begin{bmatrix} H[0] \\ H[1] \\ \vdots \\ H[N-1] \end{bmatrix} + \begin{bmatrix} Z[0] \\ Z[1] \\ \vdots \\ Z[N-1] \end{bmatrix}$$

where H is a channel vector given as $H = [H[0], H[1], ..., H[N-1]]^T$ and Z is a noise vector given as $Z = [Z[0], Z[1], ..., Z[N-1]]^T$ with E[Z[k]] = 0 and $Var[Z[k]] = \sigma_z^2$, $k = 0, 1, 2, ..., N-1$.

4.3 Estimation Techniques

There exists several techniques for estimation of channel but considering their computational complexity and nature of the channel following are more popular than others,

1. Least Square Estimator
2. Minimum Mean Square Estimator

4.3.1 Least Square Estimate

Least square (LS) channel estimation methods finds the channel estimate $\hat{H}$ in such a way that the following cost function is minimized:

$$\begin{aligned} J(\hat{H}) &= ||Y - X\hat{H}||^2 \\ &= (Y - X\hat{H})^H (Y - X\hat{H}) \\ &= Y^H Y - Y^H X\hat{H} - \hat{H}^H X^H Y + \hat{H}^H X^H X\hat{H} \end{aligned} \tag{4.1}$$

By setting the derivative of the function with respect to $\hat{H}^H$ to zero,

$$\frac{\partial J(\hat{H})}{\partial \hat{H}^H} = -(X^H Y) + (X^H X\hat{H}) = 0$$

we have $X^H X\hat{H} = X^H Y$, which gives the solution to the LS channel estimation as

$$\hat{H}_{LS} = (X^H X)^{-1} X^H Y = X^{-1} Y$$

Lets consider the LS estimate of the channel for each subcarrier as $\hat{H_{LS}}[k], k = 0, 1, 2.....N-1$. Since X is a diagonal matrix because of no ICI, the LS estimate $\hat{H_{LS}}$ can be written for each subcarrier as

$$\hat{H}_{LS}[k] = \frac{Y[k]}{X[k]}, k = 0, 1, 2, ..., N-1$$

4.3.2 LS Estimation for STBC OFDM System

The extension of LS estimate for STBC OFDM systems as described in [9] which gives the method to find the channel estimate of the system having multiple transmitters and receiver antennas. In the following section we define the STBC- OFDM system and channel statistics used for estimation.

STBC-OFDM System

In this estimation problem we consider the STBC system having N_T transmitter antennas and N_R receiver antennas. The OFDM symbol at the k^{th} subcarrier $k = 0, 1, 2, \cdots, N-1$ from the i^{th} transmitter antenna, $i = 0, 1, 2, \cdots, N_T$ is denoted by $x_i[n, k]$. Now OFDM symbols undergoes basic OFDM processing and simultaneously transmitted from corresponding antenna. We assume the channel to be quasi-static, i.e. it remains constant during the transmission of one OFDM symbol. Now at the receiver we define the received signal of K^{th} subcarrier at the j^{th} receiver antenna at time instant n as $r_j[n, k]$, $r_j[n, k]$ equals,

$$r_j[n, k] = \sum_{i=1}^{N_T} H_{ij}[n, k] x_i[n, k] + w_j[n, k]$$

where $H_{ij}[n, k]$ denotes the normalized channel frequency response for the k^{th} subcarrier at time n, corresponding to the channel between i^{th} transmitter and j^{th} receiver antenna. $w_j[n, k]$ denotes the additive complex white Gaussian noise at the receiver antenna j for k^{th} subcarrier.

Channel Model

The complex response of the channel in time domain between the i^{th} transmitter and j^{th} receiver antenna is represented by

$$h_{ij}(t,\tau) = \sum_{l} \alpha_l(t)\delta(t-\tau_l) \tag{4.2}$$

where τ_l is the time delay of the l^{th} path and $\alpha_l(t)$ denotes the complex amplitude of the l^{th} path at time instant t. Thus we can define the frequency response of the channel as

$$H_{ij}[k] = \sum_{l=0}^{L-1} h_{ij}[l]F_K^{kL} \tag{4.3}$$

where $h_{ij}[l]$ is the channel impulse response at l^{th} path between i^{th} transmitter and j^{th} receiver and $F_K = \frac{1}{\sqrt{k}}e^{\frac{-j2\pi}{K}}$, L is the total number of non-zero paths between transmitter and receiver.

System Definition

For Channel estimation in STBC-OFDM system following parameters and matrices has to be defined,

$$r[n] = (r[n,0], r[n,1], \cdots, r[n,K-1])^T \tag{4.4}$$

,

$$X[n] = (x_1[n], x_2[n], \cdots, x_{N_T}[n]) \tag{4.5}$$

where $x_i[n]$ will be a diagonal matrix , $diag(x_i[n,0], x_i[n,1], \cdots, x_i[n,K-1])$ H is the frequency response of the channel, in a matrix form it is defined as

$$H = (H_1^T, H_2^T, \cdots, H_{N_T}^T)^T \tag{4.6}$$

where $H_i = (H_i[0], H_i[1], \cdots, H_i[k-1])^T$

h is the impulse response of the channel in time domain is denoted as,

$$h = (h_1^T, h_2^T, \cdots, h_{N_T})^T \tag{4.7}$$

where h_i will be equal to number of taps in the channel or say paths consider in the channel for i^{th} transmitter which is equal to $h_i = (h_i[0], h_i[1], \cdots, h_i[L-1])^T$

$w[n]$ is the complex additive white Gaussian noise defined for every time instant and at each subcarrier,

$$w[n] = (w[n,0], w[n,1], \cdots, w[n,k-1])^T \tag{4.8}$$

W is defined as diagonal matrix of size $N_T k \times N_T l$,

$$W = \begin{bmatrix} F & 0 & \cdots & 0 \\ 0 & F & \cdots & 0 \\ \vdots & \vdots & \ddots & \vdots \\ 0 & 0 & \cdots & F \end{bmatrix}$$

where $F_{pq} = F_K^{(p-1)(q-1)}$ for $1 \leq p \leq K, 1 \leq q \leq L$. The F matrix we have defined will be of size $K \times$ Ł but since we are using comb type pilot arrangement for channel estimation we will only be needing the rows in F corresponding to pilot position. Now according to the above given equations and matrices we can define the system equation at the receiver for the STBC OFDM system as,

$$\begin{aligned} r[n] &= X[n]H + w[n] \\ &= X[n]Wh + w[n] \end{aligned} \tag{4.9}$$

LS Estimation

According to the system equations and matrices defined in previous section we can calculate LS estimate of the channel in STBC OFDM system by minimizing the cost function defined as $(r[n] - X[n]Wh)^H(r[n] - X[n]Wh)$ which gives the LS estimate $\hat{h}$ as,

$$\hat{h} = (W^H X[n]^H X[n]W)^{-1} W^H X[n]^H r[n] \tag{4.10}$$

$\hat{h}$ is the impulse response of the channel in time domain, to get the frequency response corresponding to the estimated channel we have to multiply it by W matrix defined above.

4.3.3 MMSE Channel Estimation

The LS Estimation method discussed earlier will give the channel estimates that minimizes the least square error in a particular OFDM symbol. The MMSE channel estimation will find the minimum mean square estimate for the entire transmission sequence by exploiting the spaced frequency correlation property.

System Description

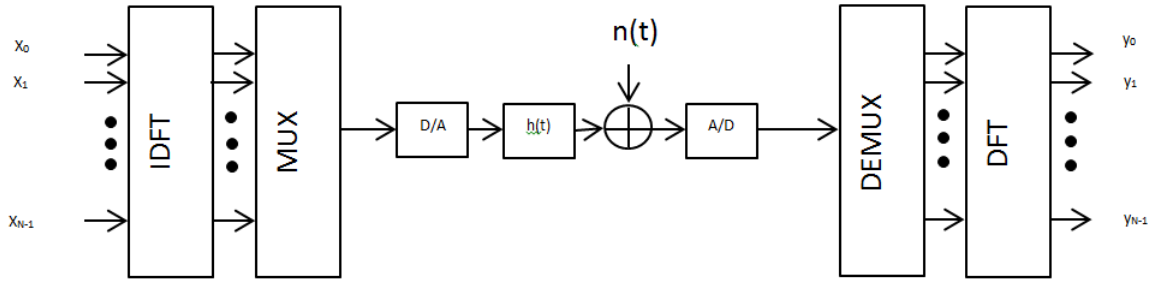

Figure 4.1: Base Band OFDM system

Consider the system in Figure 4.1. x_k are the transmitted symbols, $h(t)$ is the channel impulse response, y_k are the received symbols and $n(t)$ is the white complex Gaussian channel noise. x_k are the symbol outputs from a signal mapper like QAM or PSK. The D/A and A/D converters contain ideal low-pass filters with bandwidth $1/T_s$, where T_s, is the sampling interval. We are not looking at the insertion of cyclic prefix at this juncture, as it unnecessarily increases the system complexity.

The channel impulse response $h(t)$ is a time limited one of length C_t and is given by:

$$h(t) = \sum_{m=1}^{C_t} \alpha_m \delta(t - \tau_m T_S) \tag{4.11}$$

Here α_m are the complex amplitudes and we assume that the entire impulse train lies within the guard interval T_g. So the system can be modelled as:

$$y = DFT(IDFT(x) \circledast h + n) \tag{4.12}$$

Which can be written in the frequency domain as:

$$\begin{aligned} Y &= XH + N \\ &= XFh + N \end{aligned} \tag{4.13}$$

Where X is a diagonal matrix and,

$$F = \begin{pmatrix} W_N^{0,0} & \cdots & W_N^{0,N-1} \\ \vdots & \ddots & \vdots \\ W_N^{N-1,0} & \cdots & W_N^{N-1,N-1} \end{pmatrix}$$

is the DFT matrix with

$$W_N^{i,j} = e^{-j2\pi \frac{ij}{N}} \tag{4.14}$$

Estimation

For a Gaussian and uncorrelated channel with impulse response given by h and channel noise, the MMSE estimate of h is given by

$$\hat{h}_{MMSE} = R_{hy} R_{yy}^{-1} y \tag{4.15}$$

where,

$$R_{hy} = E[h, y^H] = R_{hh} F_T^H X^H \tag{4.16}$$

$$R_{yy} = E[y, y^H] = X F_T R_{hh} F_T^H X^H + \sigma_n^2 I_N \tag{4.17}$$

are the cross-covariance matrix between h and y and the auto-covariance matrix of y. And R_{hh} is the auto-covariance matrix of h and σ_n^2 denotes the noise variance.

Now in this method we are using a comb type pilot arrangement. So the X matrix that is used is a diagonal matrix with the known N_p pilot symbols.

$$X = diag[X_1, X_2, ...X_{N_p}] \tag{4.18}$$

F_T is a truncated DFT matrix that we are using to reduce the complexity of the system by bringing down the number of complex multiplications. It has the first C_t columns of the original DFT matrix F and rows corresponding to the pilot locations.

4.3.4 MMSE Estimation for STBC OFDM systems

The system definition and channel model is same as that used for LS Estimation.

Estimation

The channel vector h is assumed to be a Gaussian process and uncorrelated with the channel noise $w[n]$. Therefore according to the orthogonality principle the MMSE estimate of h is given by

$$\hat{h}_{MMSE} = R_{hr[n]} R^{-1}_{r[n]r[n]} r[n] \tag{4.19}$$

where ,

$$R_{hr[n]} = E[h, r[n]^H] = R_{hh} W^H C[n]^H \tag{4.20}$$

$$R_{r[n]r[n]} = E[r[n], r[n]^H] = C[n] W R_{hh} W^H C[n]^H + \sigma_w^2 I_K \tag{4.21}$$

and R_{hh} is the auto-covariance matrix of h, which is assumed to be known. Also I_K is the K x K identity matrix.

4.4 Results

4.4.1 Simulation Parameters

- Number of subcarrier = 64
- Cyclic Prefix length = 16
- Number of channel taps = 4
- Number of pilot tones = 16
- Channel PDP = [0.8187, 0.6703, 0.5488, 0.4493]

4.4.2 MSE Performance of LS and MMSE estimators

Figure 4.2 gives the mean square error associated with the LS and MMSE channel estimation methods at various SNRs for a SISO system.

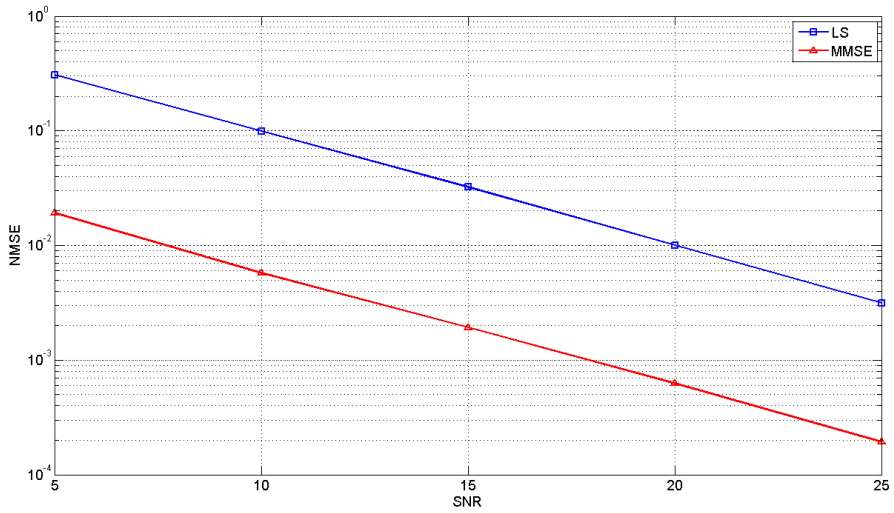

Figure 4.2: MSE Performance of LS and MMSE

Inference

We can see that MMSE out performs LS for the entire SNR range. Also as the SNR increases, both the estimates becomes more accurate.

4.4.3 SER Performance of MMSE based channel estimation for different modulation schemes

Figure 4.3 gives the symbol error rate associated with MMSE channel estimation methods at various SNRs for a SISO system for 16QAM, 8QAM and 4QAM modulation schemes.

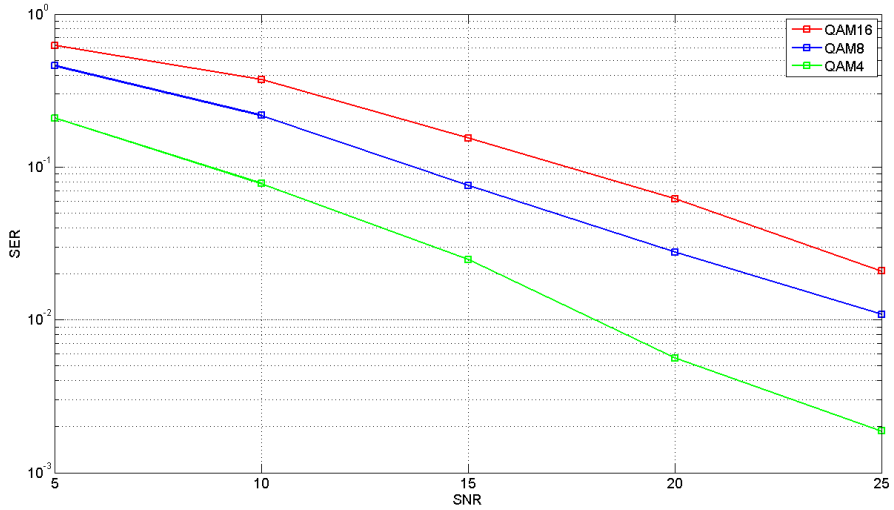

Figure 4.3: SER Performance of MMSE for different modulation schemes

Inference

Figure 4.3 shows that a lower modulation schemes gives a better SER performance. The demodulation of the received signal depends on the proximity of the constellation points. On using a higher modulation scheme the constellation points becomes closer, thus increasing the chance of a received point being incorrectly demodulated.

4.4.4 Effect of changing the number of pilots

Figure 4.4 and 4.5 gives the MSE and SER associated with the MMSE channel estimation for different number of pilots.

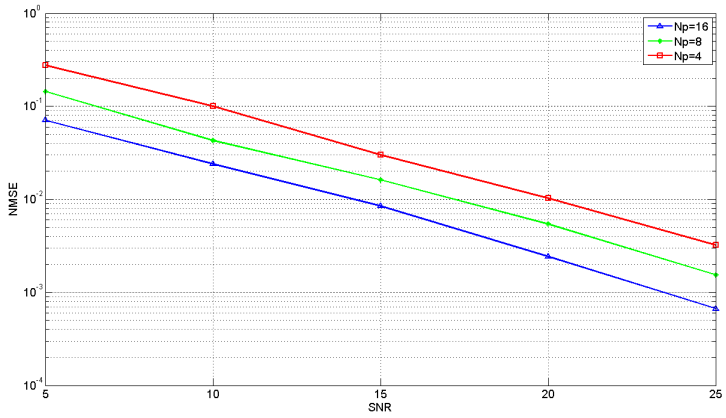

Figure 4.4: MSE Performance for different number of pilots

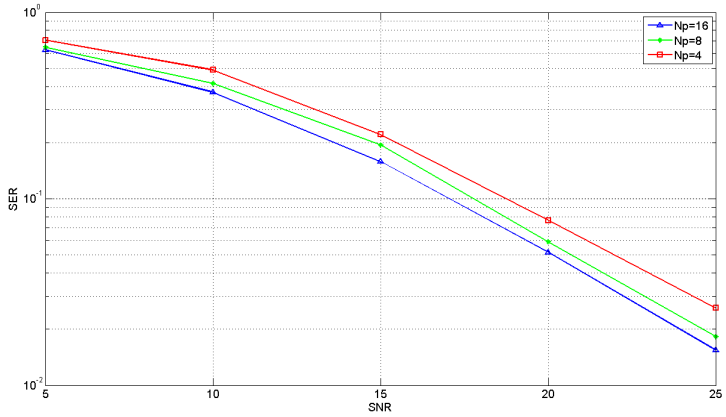

Figure 4.5: SER Performance for different number of pilots

Inference

Figure 4.4 and 4.5 shows that the performance increases as we increase the number of pilots. This is expected as we will have more reference signals to extract channel information if we increase the number of pilots.

CHAPTER 5

Kalman Filter based Channel Estimation

5.1 Introduction

MMSE and LS estimators described in previous sections assumes channel to be wide-sense stationary random process. But in reality, this assumption is incorrect because the channel can be a non-stationary process as well. Under such conditions, it is useful to use techniques like Kalman Filters for channel estimation. Kalman filter is an adaptive filter hence the estimate will track the exact value of the channel matrix as well.

5.2 Scalar Kalman Filter Problem

5.2.1 Problem Definition

Discrete time linear systems are usually described in a state variable form given by:

$$x_j = ax_{j-1} + bu_j \tag{5.1}$$

where the state, x_j, is a scalar, a and b are constants and the input u_j is a scalar; j represents the time index. Figure 5.1 gives a pictorial representation of this system, where the block with T in it represents a time delay.

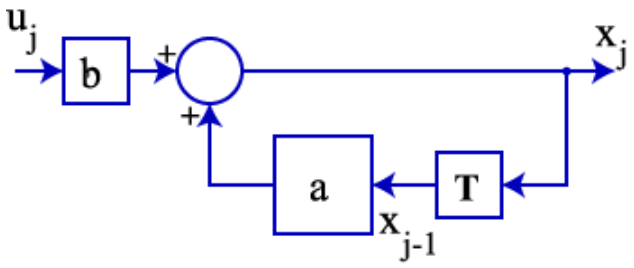

Figure 5.1: Block diagram for discrete time linear systems

Now if the system gets corrupted by noise, the system definition changes to:

$$x_j = ax_{j-1} + bu_j + w_j \tag{5.2}$$

where, w is white noise with zero mean and covariance Q and is uncorrelated with the input. The process can now be represented as shown in Figure 5.2,

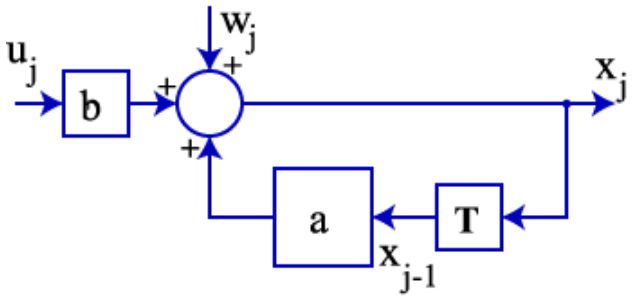

Figure 5.2: Block diagram for discrete time linear systems corrupted by noise

Now if the signal x is measured, and the measured value is z,

$$z_j = hx_j + v_j \tag{5.3}$$

The measured value z depends on the current value of x and on the gain h. The noise v is white noise. Figure 5.3 gives the present system till now.

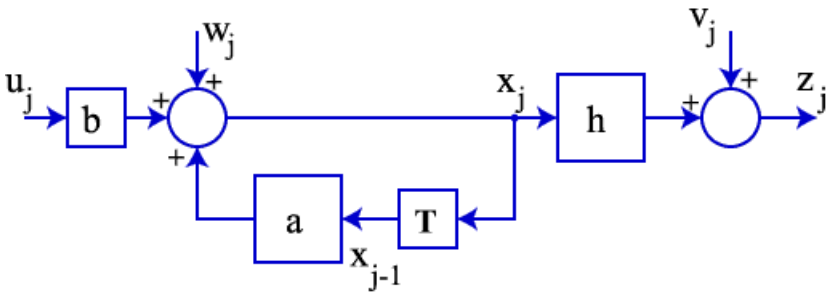

Figure 5.3: Block diagram for discrete time linear systems with the measurement

The Kalman filter problem is to filter z to get an estimate of x which minimizes the effect of both w and v.
A simple solution to the problem is to recreate the system model to get the estimate of x_j(given by $\hat{x}_j$). This is shown in Figure 5.4.

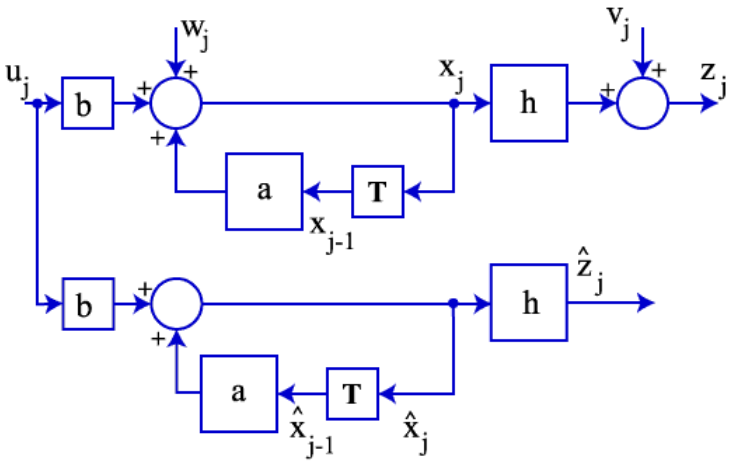

Figure 5.4: Recreating the system model

But this approach has two inherent problems. The first is that there is no correction. If we don't know the quantities a, b or h exactly (or the initial value x_0), the estimate will not track the exact value of x. Secondly, we don't compensate for the addition of the noise sources (w and v). An improved setup which takes care of both of these problems is shown in Figure 5.5.

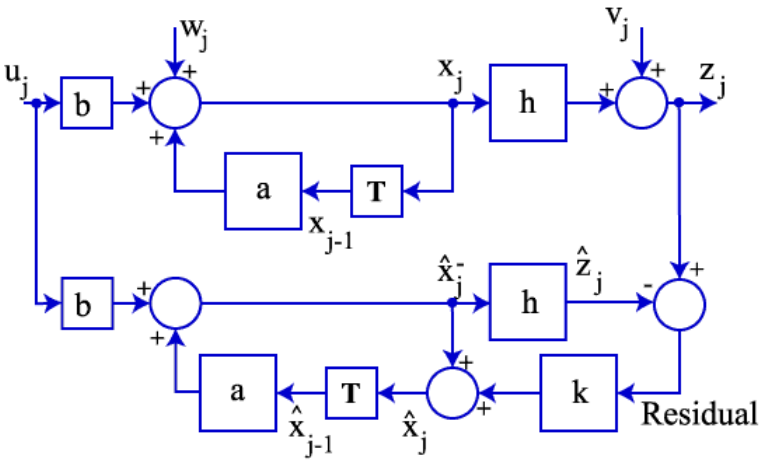

Figure 5.5: Kalman Filtering

In this approach we will first make a prediction regarding x at time j based on the information available till j-1. This is called the a priori estimate and is given by:

$$\hat{x}_j^- = a\hat{x}_{j-1} + bu_j \tag{5.4}$$

We use this a priori estimate to predict an estimate for the output, $\hat{z}_j$. The difference between this estimated output and the actual output is called the residual, or innovation.

$$Residual = z_j - \hat{z}_j = z_j - h\hat{x}_j^- \tag{5.5}$$

If the residual is small, it generally means we have a good estimate; if it is large the estimate is not so good. We can use this information to refine our estimate of x_j; we call this new estimate the a posteriori estimate, $\hat{x}_j$. If the residual is small, so is the correction to the estimate. As the residual grows, so does the correction. The entire system can be modeled as:

$$\hat{x}_j = \hat{x}_j^- + k(Residual) = \hat{x}_j^- + k(z_j - h\hat{x}_j^-) \tag{5.6}$$

The only task now is to find the quantity k that is used to refine our estimate, and it is this process that is at the heart of Kalman filtering.

5.2.2 The Kalman Gain

There are two errors which are of interest in the above problem definition. An a priori error e_j^-, and an a posteriori error e_j.

$$e_j^- = x_j - \hat{x}_j^- \tag{5.7}$$

$$e_j = x_j - \hat{x}_j \tag{5.8}$$

Associated with each of these errors is a mean squared error, or variance:

$$p_j^- = E(e_j^-)^2 \tag{5.9}$$

$$p_j = E(e_j)^2 \tag{5.10}$$

where the operator E represents the expected or average value. A Kalman filter minimizes the a posteriori variance p_j by suitably choosing the value of k.

The value for k is calculated to be,

$$k = \frac{hp_j^-}{h^2 p_j^- + R} \tag{5.11}$$

However, there is still a problem because this expression needs a value for the a priori covariance which in turn requires a knowledge of the system variable x_j. Therefore our next task will be to come up with an estimate for the a priori covariance.

But before that let's examine this equation for k. First note that the "constant", k, changes at every iteration.

5.2.3 Kalman Filtering

Any Kalman filter operation begins with a system description consisting of gains a, b and h. The state is x, the input to the system is u, and the output is z. The time index is given by j.

$$x_j = ax_{j-1} + bu_j + w_j \tag{5.12}$$

$$z_j = hx_j + v_j \tag{5.13}$$

The process has two steps, a predictor step and a corrector step.

In the predictor step, an a priori estimate of the state($\hat{x}_j^-$) and the a priori covariance(p_j^-) is calculated.

In the corrector step the Kalman gain(k) is calculated and used to refine the a priori estimate to give us the a posteriori estimate of the state($\hat{x}_j$).

Then we can calculate the a posteriori covariance which will be used in the next iteration.

5.3 Kalman Filter for Channel Estimation

In an earlier chapter we had discussed how a fading channel can be approximated by an AR model. Based on that discussion we can model a channel tap at time n by the following p^{th} order AR process.

$$h_{n,\tau} = \sum_{k=1}^{p} a_k h_{n-k,\tau} + w_{n,\tau} \tag{5.14}$$

This can be equivalently written as:

$$\begin{bmatrix} h_{n,\tau} \\ h_{n-1,\tau} \\ \vdots \\ h_{n-p+1,\tau} \end{bmatrix} = \begin{bmatrix} a_1 & a_2 & \cdots & a_{p-1} & a_p \\ 1 & 0 & \cdots & 0 & 0 \\ \vdots & \vdots & \ddots & \vdots & \vdots \\ 0 & 0 & \cdots & 1 & 0 \end{bmatrix} \begin{bmatrix} h_{n-1,\tau} \\ h_{n-2,\tau} \\ \vdots \\ h_{n-p,\tau} \end{bmatrix} + \begin{bmatrix} 1 \\ 0 \\ \vdots \\ 0 \end{bmatrix} w_{n,\tau}$$

$$h_{n,\tau} = A_1 h_{n1k,\tau} + b w_{n,\tau} \tag{5.15}$$

In the next section we will discuss how to extend this concept to a MIMO system with an m tap channel.

5.3.1 Defining the System Matrices and Noise Covariance Matrices

For the general system with N_t transmit antennas and N_r receive antennas the state equation for the Kalman filter is given by:

$$H_n = AH_{n-1} + W_n \tag{5.16}$$

where,

$$A = \begin{bmatrix} A_1 & 0 & \cdots & 0 \\ 0 & A_1 & \cdots & 0 \\ \vdots & \vdots & \ddots & \vdots \\ 0 & 0 & \cdots & A_1 \end{bmatrix} B = \begin{bmatrix} b \\ b \\ \vdots \\ b \end{bmatrix} H_n = \begin{bmatrix} h_{n,0} \\ h_{n,1} \\ \vdots \\ h_{n,mN_tN_r} \end{bmatrix} W_n = \begin{bmatrix} bw_{n,0} \\ bw_{n,1} \\ \vdots \\ bw_{n,mN_tN_r} \end{bmatrix}$$

To construct A we first diagonally extend A_1, m times to create A_2. Then we diagonally extend A_2, N_t times to get A_3. And finally we diagonally extend A_3, N_r times to get A. So, the dimension of A will be, $A \in C^{pmN_tN_r \times pmN_tN_r}$

To construct B we column wise extend b, mN_tN_r times; likewise we extend h_n to form H_n and bw_n to form W_n.

$B \in R^{pmN_tN_r \times 1}$, $H_n \in C^{pmN_tN_r \times 1}$ and $W_n \in C^{pmN_tN_r \times 1}$,

After every state update, only the first element of h_n gives the current state. The rest of its entries are the $p-1$ past states. So we will multiply H_n with an appropriate C matrix to get the current states at every tap between every transmit and receive antennas.

The noise covariance matrix for the process noise while approximating each tap by a pth order AR model is given by:

$$Q = \begin{bmatrix} q & 0 & \cdots & 0 \\ 0 & q & \cdots & 0 \\ \vdots & \vdots & \ddots & \vdots \\ 0 & 0 & \cdots & q \end{bmatrix}$$

where $q = E[(bw_{n,\tau})(bw_{n,\tau})^H] = b\sigma_w^2 b^H$. So, $q \in R^{p \times p}$ and $Q \in R^{pmNtNr \times pmNtNr}$.

The measurement covariance matrix R is given by:

$$R = \sigma_v^2 I_{N_pN_tN_R \times N_pN_r} \tag{5.17}$$

The observation equation for this process is given by:

$$Y_n = X_nH_n + V_n = X_nF'h_n + V_n \tag{5.18}$$

$$Y_n = X_nF'CH_n + V_n \tag{5.19}$$

Where Y_n corresponds to the received signals at the pilot positions at all the N_r antennas. So, $Y_n \in C^{N_pN_r \times 1}$.

X_n is constructed by first creating x_j. x_j is a diagonal matrix with its diagonal filled with the symbols transmitted at the pilot positions from the j^{th} transmit antenna. Now we construct $X_{temp} = [x_1, x_2, ..., x_{N_t}]$. Now we diagonally extend X_{temp}, N_r times to

create X_n.

C is constructed by diagonally extending c, mN_tN_r times.

Here c=[1 0 ... 0]$_{1\times p}$. So, $C \in R^{mN_tN_r \times pmN_tN_r}$

Now the Kalman filtering equations are given by:

$$\hat{H}_{n|n-1} = A\hat{H}_{n-1|n-1} \tag{5.20}$$

$$P_{n|n-1} = AP_{n-1|n-1}A^H + Q \tag{5.21}$$

$$\hat{H}_{n|n} = \hat{H}_{n|n-1} + K_n(Y_n - X_nF'C\hat{H}_{n|n-1}) \tag{5.22}$$

$$P_{n|n} = (I - K_nX_nF'C)P_{n|n-1} \tag{5.23}$$

$$K_n = P_{n|n-1}C^HF'^HX_n^H[X_nF'CP_{n|n-1}C^HF'^HX_n^H + R]^{-1} \tag{5.24}$$

The Kalman filter requires an initial estimate of the state and an initial error covariance matrix to start the recursive process. The initial state estimate is given by an LS estimation to fill the matrix $\hat{H}_{n-1|n-1}$ in the above equations. $P_{n-1|n-1}$ is initialized as an identity matrix.

5.4 Results

5.4.1 SISO Systems

Simulation Parameters

- Number of sub carriers = 64
- N_p = 16
- Cyclic prefix length = 16
- Channel Length = 6

MSE Performance

Figure 5.6 compares the MSE performance of LS and Kalman estimation techniques.

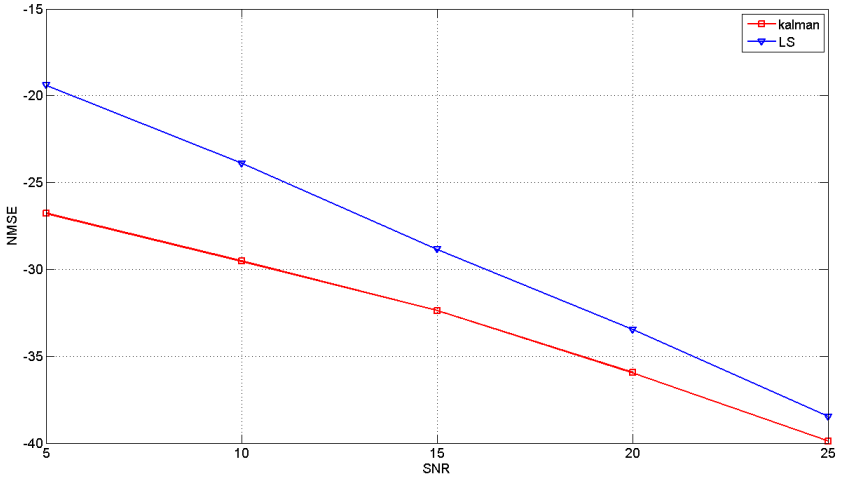

Figure 5.6: MSE performance of LS and Kalman estimation techniques

Inference

From Figure 5.6 we can clearly see that Kalman outperforms LS and gives a 6 dB improvement at low SNR.

5.4.2 MISO Systems

Simulation Parameters

- $N_t = 2$
- $N_r = 1$
- Number of sub carriers = 64
- $N_p = 16$
- Cyclic prefix length = 16
- Channel Length = 6

MSE Performance

Figure 5.7 compares the MSE performance of LS and Kalman estimation techniques.

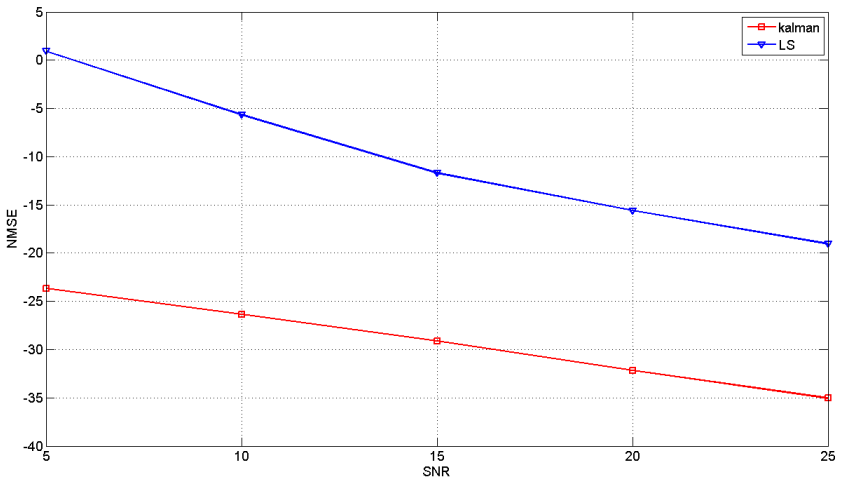

Figure 5.7: MSE performance of LS and Kalman estimation techniques

Inference

From Figure 5.7 we can clearly see that Kalman outperforms LS throughout the SNR range.

BER Performance

Figure 5.8 compares the BER performance of LS, Kalman estimation techniques along with the perfect channel estimates for 16 QAM modulation.

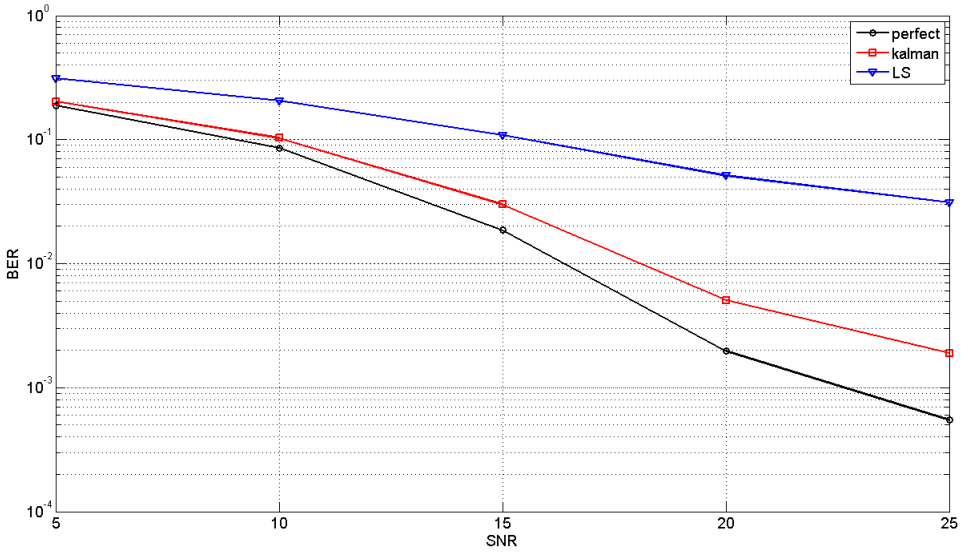

Figure 5.8: BER performance comparison(16QAM)

Inference

From Figure 5.8 we can clearly see that Kalman gives a better performance than LS and gives results near to perfect channel estimates.

BER Performance

Figure 5.9 compares the BER performance of LS, Kalman estimation techniques along with the perfect channel estimates for QPSK modulation.

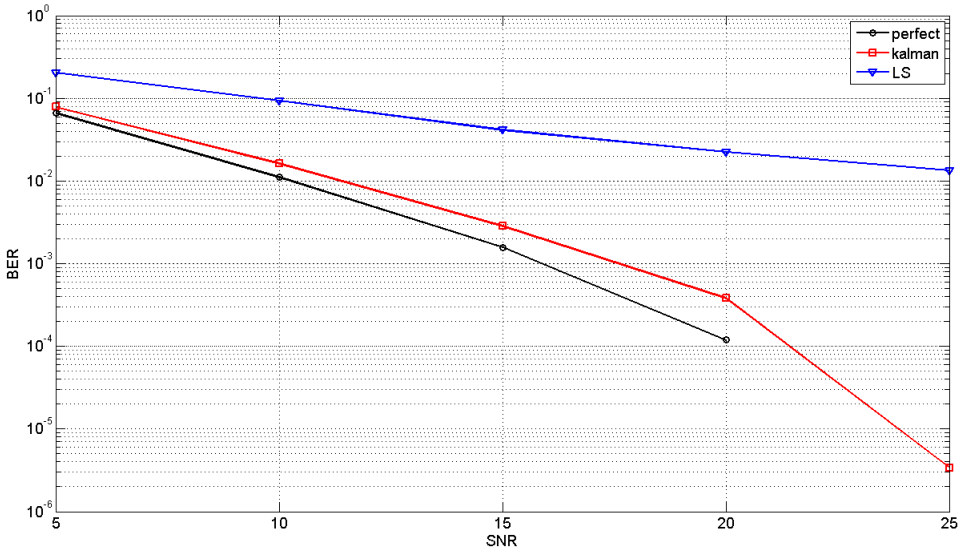

Figure 5.9: BER performance comparison(QPSK)

Inference

From Figure 5.9 we can see that Kalman still performs better than LS.

5.4.3 MIMO Systems

Simulation Parameters

- $N_t = 2$
- $N_r = 2$
- Number of sub carriers = 64
- $N_p = 16$
- Cyclic prefix length = 16
- Channel Length = 6

MSE Performance

Figure 5.10 compares the MSE performance of LS and Kalman estimation techniques.

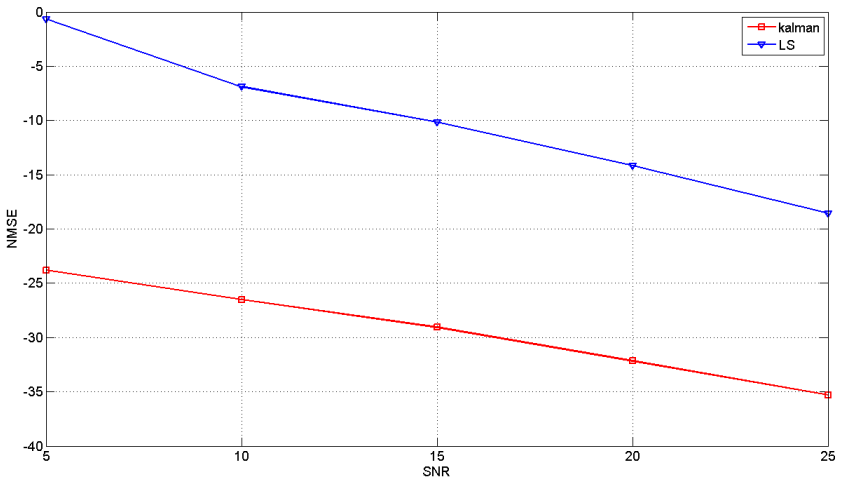

Figure 5.10: MSE performance of LS and Kalman estimation techniques

Inference

From Figure 5.10 we can clearly see that Kalman outperforms LS throughout the SNR range. And Kalman gives a 15 to 20 dB better performance than LS.

BER Performance

Figure 5.11 compares the BER performance of LS, Kalman estimation techniques along with the perfect channel estimates for 16 QAM modulation.

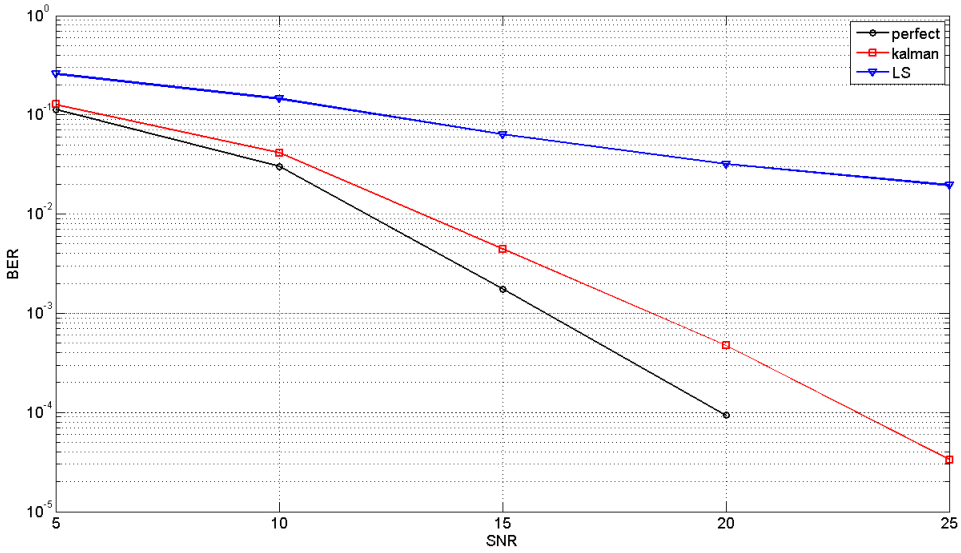

Figure 5.11: BER performance comparison(16QAM)

Inference

From Figure 5.11 we can clearly see that Kalman performs better than LS and gives results near to perfect channel estimation.

BER Performance of LS vs Kalman for QPSK

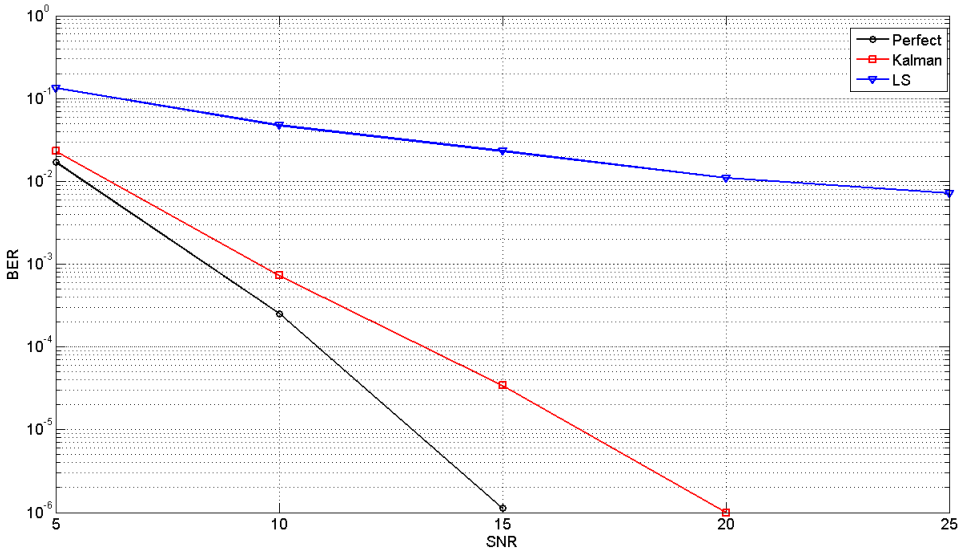

Figure 5.12: BER performance comparison(QPSK)

Kalman Channel Tracking

Figure 5.13 show us how the Kalman filter tracks the channel with time.

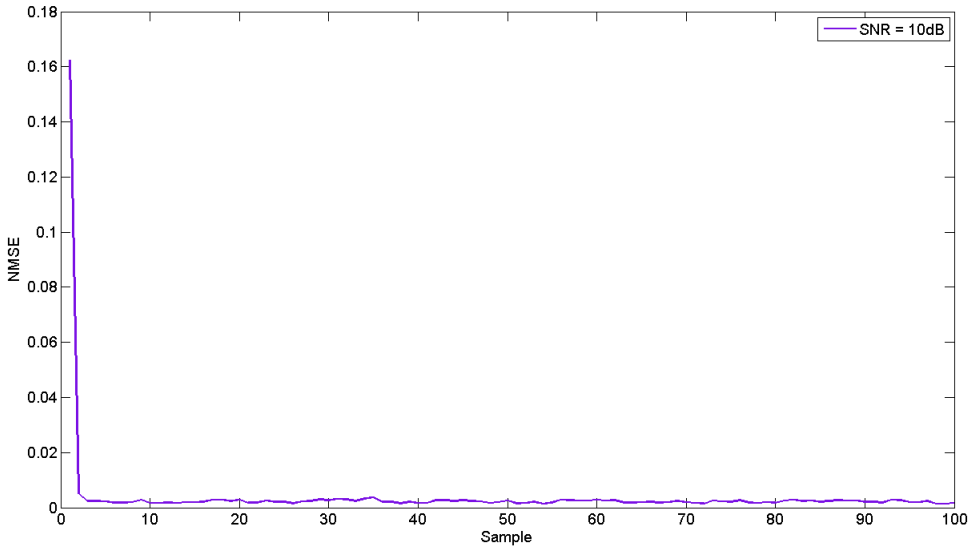

Figure 5.13: Kalman Channel Tracking

Inference

As we can see from Figure 5.13 the channel estimates given by the Kalman filter improves with time. The initial estimate is erroneous, but as time progresses the estimates become more accurate.

CHAPTER 6

Conclusions and Future Work

This chapter presents the conclusions drawn from the project and future work that could be done to increase the scope and improve upon the proposed system.

6.1 Results and Conclusions

Implementing an iterative channel estimation technique(Kalman Filtering) for STBC OFDM systems was the objective of this project.

We started by first studying the STBC OFDM systems. Simulation results for different number of transmit and receive antennas were obtained. Improvement in BER performance due to changes in modulation scheme, number of antennas and code rate was noted.

All the simulations were conducted in a Rayleigh Fading Channel. So, as the next step, the general fading channel and the methods to generate fade variables were studied. Simulations results for different doppler shifts were obtained. The AR model approximation for the fading channel was also studied as this was an integral part of the Kalman Filter. Simulations for AR approximations were done for different orders and the difference between the actual channel and AR channel was noted.

Then the existing channel estimation techniques were studied. First we implemented these techniques for SISO OFDM systems. Simulation results for MSE and BER performance were obtained. Effect of changing the modulation scheme and number of pilots was studied. Then comparisons were made after implementing Kalman Filtering for channel estimation. The proposed estimation gives a 6 dB performance improvement over the existing methods at low SNR.

After that the concept of Kalman Filtering was extended to STBC OFDM systems. Simulation results comparing MSE and BER performances of the proposed estimation technique(Kalman) and existing estimation technique(LS) was obtained. An MSE performance improvement of 15 to 20 dB was noted. BER performances very near to perfect channel estimates were obtained. Effect on BER performance due to changes in modulation scheme and number of antennas was noted.

6.2 Future Work

The scope for research in wireless communications is vast and full of endless possibilities. In this project we focused on implementing Kalman Filter based channel estimation for STBC OFDM systems. Although we have successfully completed the objective for this project, there remains further works that could be done to improve the performance of the system and bring the simulation parameters closer to realistic conditions.

6.2.1 Adaptive Modulation for Pilots and Data Subcarriers

For getting the best performance through the channel, the modulation schemes used for the data and pilots should adapt with the changes in the channel. The system should

adapt the modulation scheme to suit the present condition so as to maximise channel capacity. Simulation results in this project has shown that there is a performance improvement of 1 to 3 dB when a lower order modulation scheme is used. The selection is based on balancing the need for higher rate with that of the error threshold the system can manage. A feedback bit can be sent from the receiver to transmitter giving the state of the channel. And this feedback should use a low order modulation scheme because it is crucial that this feedback information must have minimum error.

6.2.2 Adaptive MIMO Implementation

In this project we have used STBC for MIMO Implementation throughout the transmission sequence. STBC is a technique that is useful for increasing the reliability of the transmitted data. But this reliability is achieved by transmitting redundant data which has a severe impact on the data rate of the system. So based on the channel condition if the communication system shift between STBC and Spatial Multiplexing for MIMO implementation there will be a significant improvement in terms of data rate. This needs a feedback matrix from the receiver which implements STBC at the transmitter if the channel conditions are bad and spatial multiplexing if the conditions are good.

6.2.3 Non Sample Spaced Channels

For all the simulations in this project, we have used sample spaced channels. A sample spaced channel is one which has an impulse response with path gains at integral multiples of sample time. But in the real world scenario this is not the case. Channel impulse responses with fractional delays are more common. So to bring these simulations closer to the real world conditions we can run these simulations for non sample spaced channel. For running these simulations we have to first convert the non sample spaced channel to sample spaced channel by sinc interpolation. But this leads to the impulse response spreading to FFT length in time domain. Hence the concept of cyclic prefix fails and there will be severe ISI which degrades the system performance. Hence the estimation algorithm and transmission model should be changed accordingly for these simulations.

References

[1] Yong Soo Cho, Jaekwon Kim, Won Young Yang, and Chung-Gu Kang, "MIMO-OFDM Wireless Communications with MATLAB," in *John Wiley & Sons (Asia) Pte Ltd*, 2010, pp. 129-193

[2] Anibal Luis Intini, "Orthogonal Frequency Division Multiplexing for Wireless Networks," in *University of Santa Barbara*, Dec. 2000, pp. 1-10

[3] Charan Langton, "Orthogonal Frequency Division Multiplexing(OFDM) Tutorial," in *Intuitive Guide to Principle of Communication*, 2004, pp. 1-22

[4] S. M. Alamouti, "simple transmitter diversity scheme for wireless communications," in *IEEE J. Select. Areas Commun., vol. 16*, Oct. 1998, pp. 1451-1458

[5] Mohinder Jankiraman, "Space-Time Codes and MIMO Systems," in *Artech House Universal Personal Communications Series*, 2004, pp. 75-102

[6] Vahid Tarokh, Hamid Jafarkhani, and A. Robert Calderbank, "Space-Time Block Coding for Wireless Communications: Performance Results," in *IEEE J. Select. Areas Commun., vol. 17*, March 1999, pp. 451-460

[7] M. J. Dehghani, R. Aravind and K. M. M. Prabhu, "Space-Time Block Coding in OFDM systems," in *Dept. of EE, IITM*, pp. 1-5

[8] Ilkka Harjula, and Aarne Mammela, "Channel Estimation Algorithm for Space-Time Block Coded OFDM Systems," in *Global Telecommunications Conference, 2003. GLOBECOM '03. IEEE*, 2003, pp. 143-147

[9] Papoulis, A., "Probability, Random Variables and Stochastic Processes," in *3rd Edition, McGraw Hill, New York*, 1991

[10] Rappaport Theodore S., "Wireless Communications: Principles And Practice," in *2nd Edition,Pearson Education, India*, 2010

[11] Young, D. J., Beaulieu, N. C., "The Generation of Correlated Rayleigh Random Variates by Inverse Discrete Fourier Transform," in *IEEE Transactions on Communications, vol. 48*, July 2000, pp. 1114-1127

[12] Kareem E. Baddour, and Norman C. Beaulieu, "Autoregressive Models for Fading Channel Simulation," in *Wireless Communications, IEEE Transactions, vol. 4*, 2001, pp. 1187-1192

[13] Monson H. Hayes, "Statistical Digital Signal Processing And Modeling," in *John Wiley & Sons (Asia) Pte Ltd*, 2008

[14] Jan-Jaap van de Beek, Ove Edfors, Magnus Sandell, Sarah Kate Wilson and Per Ola Borjesson, "On Channel Estimation in OFDM Systems," in *Vehicular Technology Conference, IEEE 45th vol. 2* , 1995, pp. 815-819

[15] Shuangchun Liang, and Weiling Wu, "Channel estimation based on pilot subcarrier in space-time block coded OFDM system," in *Communication Technology Proceedings, ICCT 2003. vol. 2* , 2003, pp. 1795-1798

[16] Yi Gong, and Letaief, K.B., "Low rank channel estimation for space-time coded wideband OFDM systems ," in *Vehicular Technology Conference, IEEE VTS 54th vol. 2* , 2001, pp. 772-776

[17] Yi Gong, and Letaief, K.B., "Low Complexity Channel Estimation for SpaceTime Coded Wideband OFDM Systems ," in *IEEE TRANSACTIONS ON WIRELESS COMMUNICATIONS, VOL. 2,* , 2003, pp. 876-882

[18] Kukajini Pirabakaran, and R.M.A.P. Rajatheva, "PILOT SEQUENCE AIDED CHANNEL ESTIMATION FOR SPACE TIME CODED OFDM SYSTEMS ," in *Electrical and Computer Engineering, 2005. Canadian Conference,* , 2005, pp. 896-899

[19] Greg Welch, and Gary Bishop, "An Introduction to the Kalman Filter," in *SIGGRAPH*, 2008

[20] SM Bozic, "Digital and Kalman filtering : an introduction to discrete-time filtering and optimum linear estimation," in *Halstead Press*, 1994

[21] R.Lakshminarayanan, R.Vinod and K. Giridhar, "Design of Channel Estimation and Tracking Algorithms for OFDMA Systems," in *IETE 2010*, 2010

[22] Yun Wu, and Hanwen Luo, "Channel Estimation for MIMO OFDM Systems in Non sample spaced Multipath Channels" in *Congress on Image and Signal Processing*, 2008, pp. 88-92